

NACA TN 2136

3, N 21/5: 6/2136

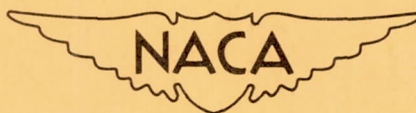
# NATIONAL ADVISORY COMMITTEE FOR AERONAUTICS

TECHNICAL NOTE 2136

THEORY OF HELICOPTER DAMPING IN PITCH OR ROLL AND A  
COMPARISON WITH FLIGHT MEASUREMENTS

By Kenneth B. Amer

Langley Aeronautical Laboratory  
Langley Air Force Base, Va.



Washington  
October 1950

BUSINESS, SCIENCE  
& TECHNOLOGY DEPT.

CONN. STATE LIBRARY

OCT 20 1950



NATIONAL ADVISORY COMMITTEE FOR AERONAUTICS

TECHNICAL NOTE 2136

THEORY OF HELICOPTER DAMPING IN PITCH OR ROLL AND A  
COMPARISON WITH FLIGHT MEASUREMENTS

By Kenneth B. Amer

SUMMARY

Calculations and flight-test measurements on a single-main-rotor helicopter indicate that the damping moment about the helicopter center of gravity produced during pitching or rolling by a rotor which has flapping hinges on the rotor shaft depends primarily upon four quantities: rotor speed, blade mass factor, height of the rotor hub above the helicopter center of gravity, and the ratio of collective pitch to the thrust coefficient - solidity ratio  $\left(\frac{\theta}{C_T/\sigma}\right)$ . The damping moment per unit angular velocity varies inversely with rotor speed and blade mass factor, varies directly with hub height, and decreases linearly with increasing  $\frac{\theta}{C_T/\sigma}$ . At values of  $\frac{\theta}{C_T/\sigma}$  above about 3, when  $\theta$  is in radians, the rotor moment per unit angular velocity becomes unstable (moment in the same direction as the angular velocity). These results indicate that present-day helicopters with conventional control systems tend to have low damping at high speeds and in climbs and that unstable damping can occur during maneuvers in which the normal acceleration falls well below 1 g.

These results also indicate that high-speed high-powered helicopters and those convertible aircraft, the lifting rotors of which have flapping hinges and are used for high-speed propulsion, may have intolerable amounts of unstable rotor damping (because of the necessarily high values of  $\frac{\theta}{C_T/\sigma}$ ) unless special design features, such as offset flapping hinges or a rate gyroscope applying opposite cyclic feathering proportional to the angular velocity are used.

This investigation also shows that the use in damping calculations of the assumption that the rotor-force-vector tilt is equal to the tip-path-plane tilt during pitching or rolling may give results which are highly misleading.

## INTRODUCTION

When a helicopter is undergoing a rolling or pitching velocity, the rotor normally produces an opposing moment about the helicopter center of gravity because the rotor-force vector lags behind its trim position with respect to the shaft. This moment is known as "damping in pitch" or "damping in roll," depending upon the axis about which it occurs. When a helicopter has insufficient rotor damping, it will have excessive control sensitivity (rate of roll per inch of control-stick deflection). The importance of adequate rotor damping was discussed in reference 1, which states that excessive lateral-control sensitivity, in hovering, can lead to overcontrolling which results in a short-period, pilot-induced, lateral oscillation. In forward flight, there is probably also a minimum amount of damping in roll (as well as damping in pitch) below which the pilot would find the helicopter difficult to control. If the damping were unstable (the rotor moment in the same direction as the angular velocity), the helicopter would be even more difficult and perhaps even impossible to control.

The source of rotor damping is illustrated in figure 1, which shows a helicopter rolling to the right. Inasmuch as the blades are hinged to the shaft, the shaft cannot physically force the blades to follow it. The tip-path plane therefore lags behind its trim position with respect to the shaft at an angle such that the cyclic air forces on the blades produced by the tip-path-plane tilt force the blades to follow the shaft. A more detailed discussion of this phenomenon is given in reference 2. If the rotor-force vector is assumed to act perpendicular to the tip-path plane (an assumption usually made for convenience), the rotor damping moment which depends upon the tilt of the force vector is always calculated to be stable, inasmuch as the tip-path plane always tilts with respect to the shaft in a direction opposite to the pitching or rolling velocity. Of course, damping moments calculated from this assumption would be incorrect if the assumption were incorrect. Because of the practical importance of the damping moment contributed by the rotor, an investigation has been made to determine in a more exact manner the change in the direction of the rotor-force vector due to a pitching or rolling velocity. The configuration considered is the single-rotor helicopter with conventional control system and flapping hinges on the rotor shaft.

## SYMBOLS

W            gross weight of helicopter, pounds  
R            blade radius, feet

- $r$  radial distance to blade element, feet  
 $b$  number of blades per rotor  
 $c$  blade-section chord, feet  
 $c_e$  equivalent blade chord (on thrust basis), feet  $\left( \frac{\int_0^R cr^2 dr}{\int_0^R r^2 dr} \right)$   
 $\sigma$  rotor solidity  $(bc_e/\pi R)$   
 $\theta$  blade-section pitch angle, angle between line of zero lift of blade section and plane perpendicular to axis of no feathering (sometimes referred to as collective pitch), radians  
 $I_1$  mass moment of inertia of blade about flapping hinge, slug-feet<sup>2</sup>  
 $\gamma$  mass constant of rotor blade; expresses ratio of air forces to inertia forces  $(c_e \rho a R^4 / I_1)$   
 $\rho$  mass density of air, slugs per cubic foot  
 $V$  true airspeed of helicopter along flight path, feet per second  
 $\Omega$  rotor angular velocity, radians per second  
 $\alpha$  rotor angle of attack; angle between flight path and plane perpendicular to axis of no feathering, positive when axis is pointing rearward, radians  
 $\mu$  tip-speed ratio  $\left( \frac{V \cos \alpha}{\Omega R} \right)$   
 $v$  induced inflow velocity at rotor (always positive), feet per second  
 $\lambda$  inflow ratio  $\left( \frac{V \sin \alpha - v}{\Omega R} \right)$   
 $\psi$  blade azimuth angle measured from downwind position in direction of rotation, radians  
 $U_T$  component at blade element of resultant velocity perpendicular to blade-span axis and to axis of no feathering, feet per second

- $U_P$  component at blade element of resultant velocity perpendicular both to blade-span axis and  $U_T$ , feet per second
- $\phi$  inflow angle at blade element in plane perpendicular to blade-span axis, radians  $\left(\tan^{-1} \frac{U_P}{U_T}\right)$
- $\alpha_r$  blade-element angle of attack, measured from line of zero lift, radians  $(\theta + \phi)$
- $a$  slope of curve of section lift coefficient against section angle of attack in radians
- $T$  rotor thrust (component of rotor force parallel to axis of no feathering), pounds
- $C_T$  rotor thrust coefficient  $\left(\frac{T}{\pi R^2 \rho (\Omega R)^2}\right)$
- $L$  lift, pounds
- $C_L$  rotor lift coefficient  $\left(\frac{L}{\frac{1}{2} \rho V^2 \pi R^2}\right)$
- $Y$  lateral force (component of rotor force perpendicular both to the flight path and to the axis of no feathering), pounds
- $C_Y$  rotor lateral-force coefficient  $\left(\frac{Y}{\pi R^2 \rho (\Omega R)^2}\right)$
- $B$  tip-loss factor; blade elements outboard of radius  $BR$  are assumed to have profile drag but no lift
- $\beta$  blade-flapping angle at particular azimuth position  
 $(\beta = a_0 - a_1 \cos \psi - b_1 \sin \psi \dots)$
- $a_0$  constant term in Fourier series that expresses  $\beta$ , radians; hence, rotor coning angle
- $a_1$  coefficient of  $-\cos \psi$  in expression for  $\beta$ ; hence, longitudinal tilt of rotor cone with respect to axis of no feathering, positive for rearward tilt
- $b_1$  coefficient of  $-\sin \psi$  in expression for  $\beta$ ; hence, lateral tilt of rotor cone with respect to axis of no feathering, positive for right tilt

- a' projection of angle between rotor resultant force vector and axis of no feathering in plane containing flight path and axis of no feathering
- b' projection of angle between rotor resultant force vector and axis of no feathering in the plane containing the axis of no feathering and perpendicular to the plane containing flight path and axis of no feathering
- $\Delta$  increment
- p angular velocity of the helicopter in roll, positive for right roll, radians per second
- q angular velocity of the helicopter in pitch, positive for nose-up pitching, radians per second
- t time, seconds

#### THEORETICAL ANALYSIS

The first step in the determination of rotor damping is to calculate the change in longitudinal and lateral flapping (tip-path-plane tilt) due to a pitching or rolling velocity. Once this step is completed, the change in rotor-force-vector direction and hence the damping moment can be calculated.

During steady pitching or rolling, the rotor blades, like any rotating mass, must be continuously accelerated in order to tilt the tip-path plane; thus, inertia forces will be acting on the blades. If the helicopter has a steady pitching velocity  $q$  and a steady rolling velocity  $p$ , the inertia forces produce a moment about the flapping hinge equal to

$$-2q\Omega I_1 \sin \psi + 2p\Omega I_1 \cos \psi \quad (1)$$

Equation (1) is derived in a manner similar to the derivation, in appendix 2 of reference 3, of the inertia moment acting on a tilting gyroscope. The two terms of equation (1) are added to the right side of equation (9-8) of reference 4 (which is the equation of moments about the flapping hinge). Then, by the procedure used to obtain equations (9-11) of reference 4, the following results are obtained for the tilt of the tip-path plane with respect to the shaft due to a steady pitching or rolling velocity (changes in second harmonic flapping being neglected):

$$\frac{\Delta b_1}{p} = -\frac{16/B^4}{\gamma\Omega\left(1 + \frac{\mu^2}{2B^2}\right)} \quad (2)$$

$$\frac{\Delta a_1}{q} = -\frac{16/B^4}{\gamma\Omega\left(1 - \frac{\mu^2}{2B^2}\right)} \quad (3)$$

Equations (2) and (3) confirm the previous statement that the tilt of the tip-path plane is in a direction opposite to the angular velocity. As would be expected, at  $\mu = 0$  the lateral flapping due to rolling is equal to the longitudinal flapping due to pitching. The effect of tip-speed ratio is quite small and causes a change of only 13 percent from  $\mu = 0$  to  $\mu = 0.50$ . The tip-path-plane tilt per unit angular velocity is inversely proportional to  $\gamma$  and  $\Omega$ . Inasmuch as  $\gamma$  and  $\Omega$  are relatively constant for a given helicopter, the tip-path-plane tilt per unit angular velocity is relatively independent of flight condition.

Now that the changes in flapping are known, the change in direction of the rotor-force vector can be calculated. The calculation is carried out for the helicopter during roll at  $\mu = 0$  (hovering or vertical flight). The first step in the procedure consists in setting up the equation for the lateral force  $Y$  (component of rotor force perpendicular both to the flight path and to the axis of no feathering).

Figure 2, which is a schematic plan view of the helicopter rotor, shows the contribution of the lift on a blade element to the lateral force  $Y$  to be (if  $\phi$  and  $\beta$  are assumed to be small angles)

$$dY = \phi dL \cos \psi - \beta dL \sin \psi \quad (4)$$

where  $dL$  is the lift acting on the blade element. The spanwise component of lift  $\beta dL$  is caused by the flapping angle  $\beta$ ; inasmuch as the lift acts perpendicular to the blade-span axis. The chordwise component of lift  $\phi dL$  is due to the inflow angle  $\phi$  at the blade element. This inflow angle causes an equal angular tilt of the lift vector with respect to the axis of no feathering.

The contribution of the drag of the blade element to the lateral force is small and is neglected. When the procedure of sections 7 and 8 of reference 4 is followed and higher harmonic flapping is neglected, the following relations are obtained ( $\phi$  being assumed small):



$$\left. \begin{aligned}
 dL &= \frac{1}{2} \rho b c U^2 c_l dr \\
 c_l &= a \alpha_r \\
 \alpha_r &= \theta + \phi \\
 \phi &= \frac{U_P}{U_T} \\
 U &= U_T \\
 U_T &= \Omega r \\
 U_P &= \lambda \Omega R - r \frac{d\beta}{dt} \\
 \beta &= a_0 - a_1 \cos \psi - b_1 \sin \psi
 \end{aligned} \right\} \text{for } \mu = 0 \tag{5}$$

Substitution of equations (5) in equation (4), integrating around the rotor disk, and differentiating with respect to  $b_1$  results in

$$\frac{\Delta \left( \frac{2C_Y}{\sigma a} \right)}{\Delta b_1} = \frac{3}{2} \left( \lambda \frac{B^2}{2} + \frac{2}{9} \theta B^3 \right) \tag{6}$$

For  $\mu = 0$ , equation (8-14) of reference 4 becomes

$$\frac{2C_T}{\sigma a} = \frac{\lambda B^2}{2} + \frac{\theta B^3}{3} \tag{7}$$

From figure 3, it can be seen that the presence of a lateral force  $Y$  causes the resultant rotor-force vector to be displaced from the axis of no feathering by an angle  $b'$ . Since  $b'$  is usually a small angle, it may be written as

$$b' = \frac{Y}{T} = \frac{C_Y}{C_T}$$

Thus,

$$\frac{\Delta b'}{\Delta b_1} = \frac{\Delta C_Y / \Delta b_1}{C_T} \quad (8)$$

Substituting equations (6) and (7) in equation (8) results in the following equation:

$$\frac{\Delta b'}{\Delta b_1} = \frac{3}{2} \left( 1.0 - \frac{B^3 a}{18} \frac{\theta}{C_T / \sigma} \right)$$

For  $B = 0.97$  and  $a = 5.73$  (experience has shown these values to be sufficiently accurate over a wide range of flight conditions),

$$\frac{\Delta b'}{\Delta b_1} = \frac{3}{2} \left( 1.0 - 0.29 \frac{\theta}{C_T / \sigma} \right) \quad (9)$$

Additional calculations for forward flight show that the effect of  $\mu$  is quite small. A repeat of the calculations for the helicopter in pitch at  $\mu = 0$  yields, as would be expected, the same result as equation (9). The effect of  $\mu$  is also quite small for the helicopter in pitch.

Multiplying equations (2) and (9) gives, for  $\mu = 0$  and  $B = 0.97$ ,

$$-\frac{\Delta b'}{p} = -\frac{27}{\gamma \Omega} \left( 1.0 - 0.29 \frac{\theta}{C_T / \sigma} \right) \quad (10)$$

As discussed previously, the effect of  $\mu$  on equation (2) is small and the extension of equation (9) to cover forward flight would cause little change. Equation (10) is therefore fairly accurate for both roll and pitch for values of  $\mu \leq 0.50$ . The rotor damping moment about the helicopter center of gravity per unit angular velocity is obtained by multiplying equation (10) by the height of the rotor hub above the helicopter center of gravity and by the rotor thrust.

Equation (9) indicates that the tilt of the rotor-force vector due to a pitching or rolling velocity is not necessarily equal (even approximately) to the tilt of the tip-path plane and, hence, calculations of rotor damping based on tip-path-plane tilt may be in error. Equation (10) indicates that rotor damping is inversely proportional to blade mass factor  $\gamma$  and rotor speed  $\Omega$  and that, at values of the parameter  $\frac{\theta}{C_T / \sigma}$  below about 3, the rotor damping moment opposes the angular velocity; whereas, at values of the parameter  $\frac{\theta}{C_T / \sigma}$  above about 3, the tilt of the

rotor-force vector and, hence, the rotor moment is actually in the same direction as the helicopter's angular velocity. Thus, theory indicates that, for those flight conditions at which the value of the collective pitch (in radians) divided by the thrust coefficient-solidity ratio exceeds about 3, the rotor damping is unstable both in pitch and in roll. Under such conditions, the helicopter would probably be difficult, if not impossible, to control.

The translational velocity at the rotor hub due to pitching or rolling about the helicopter center of gravity rather than about the rotor hub adds slightly to the rotor damping, but this small effect has been neglected. The additional vertical velocities encountered by the rotor blades due to the pitching or rolling produce negligible damping and have also been neglected. This analysis has also neglected any changes in blade torsion moments produced by air forces or by offset of the blade chordwise center of gravity from the blade feathering axis.

The source of unstable rotor damping predicted by the theory under the conditions of high pitch and low mean angle of attack  $\left(\frac{C_T}{\sigma}\right)$  can be understood from an examination of figure 4, which shows views of the rotor as it would appear to an observer looking from the tail toward the nose of a helicopter operating at  $\mu = 0$  (hovering or vertical flight). Typical airfoil sections of the blades in the forward and rearward position are shown. Because of the low mean angle of attack, the downward air flow through the rotor must be large and hence the lift vectors on the blade elements would be tilted. (This tilt of the lift vectors causes induced torque.) No unbalanced lateral force is present, however, because the horizontal components of the lift vectors cancel each other. When the helicopter rolls to the left, the tip-path plane lags behind and hence tilts to the right with respect to the shaft, as discussed previously. Thus, the blade moving to the right is also moving down with respect to the shaft and hence its angle of attack and lift are increased. Similarly the blade moving to the left is moving up with respect to the shaft so its lift is reduced. These changes in lift act continuously to force the tip-path plane to follow the shaft during the roll. (As is true for the flapping of a rotor due to forward speed, the maximum flapping displacement occurs one-quarter revolution after the maximum air force.) As a result of these changes in lift, an unbalanced lateral force occurs to the left. Inasmuch as the rotor hub is above the helicopter center of gravity, the unbalanced lateral force causes a rolling moment to the left which is in the same direction as the rolling velocity and, therefore, is unstable. This unstable moment increases with increasing pitch for a given value of mean angle of attack  $\frac{C_T}{\sigma}$  (which would be caused by an increase in level-flight speed above the speed for minimum power or an increase in angle of climb) because the increasing inflow increases the tilt of the lift vectors.

At the same time during this roll, there is a stable rolling-moment contribution from the blades when in a lateral position (one-quarter of a revolution from the position shown in the figure). This stable rolling-moment contribution comes about because the lift acts perpendicular to the blade-span axis, which is tilted because of flapping when the blades are in the lateral position. This stable rolling-moment contribution is independent of flight condition. Thus, when the helicopter is rolling, it is only under the conditions of high pitch and low  $\frac{C_T}{\sigma}$  that the unstable rolling-moment contribution from the blades in the forward and rearward position overcomes the stable contribution of the blades in the lateral position.

The preceding explanation of the source of unstable damping in roll at  $\mu = 0$  also applies for forward flight and for damping in pitch.

#### EXPERIMENTAL VERIFICATION

Because of the important implications about rotor damping provided by the theory, an experimental verification in flight of the theoretical results was considered desirable and a helicopter was tested in flight for this purpose.

The helicopter used for the flight tests is shown in figure 5. The helicopter was fitted with, among other instruments, control-position recorders and a rolling-angular-velocity recorder with synchronized time scales. Only rotor damping in roll was investigated because measurements of damping in pitch are complicated by the static stability or instability of the helicopter with angle of attack. Also, inasmuch as the theory predicts only relatively small differences between damping in roll and damping in pitch, the experimental verification in flight of the damping in roll was considered sufficient. The flight technique involved trimming at various flight conditions and then displacing the cyclic pitch control laterally. The helicopter began to roll with increasing angular velocity until a maximum velocity was reached. Inasmuch as the flapping hinges of the test helicopter are on the rotor shaft, rolling moments on the helicopter can only be produced by tilting the rotor-force vector. Thus, at the time of maximum rolling velocity, the force vector must be back to its trim position, since no angular acceleration and consequently no unbalanced rolling moment is present. Therefore, at the time of maximum angular velocity, the lateral tilt of the rotor-force vector caused by the rolling velocity must be equal and opposite to the tilt caused by the displacement of the lateral cyclic control. Inasmuch as the change in lateral cyclic pitch caused by the lateral control displacement causes an equal lateral tilt of the force vector, the tilt of the vector due to damping at the time of maximum rolling velocity is also equal to the lateral cyclic pitch displacement from trim at the same time.

Sample flight records are shown in figure 6. The cyclic pitch control was first displaced laterally in one direction and then in the other in order to minimize the effects of sideslip. The use of this technique, however, does not affect the method of working up the data. The distance  $\Delta b'$  is the lateral displacement of the cyclic pitch control from trim at the time of maximum rolling velocity, and as discussed previously, this displacement is equal to the rotor-force-vector tilt due to the maximum rolling velocity  $p_{\max}$ . The magnitude of the rotor damping is indicated by the ratio of  $\Delta b'$  to  $p_{\max}$ , an increase in the ratio indicates increased rotor damping.

In order to compare the data with the theory, the data were calculated in the form of  $\frac{\Delta b'}{\Delta b_1}$  where  $\Delta b_1$  is obtained from equation (2) for a value of  $B = 0.97$ . The flight values of  $p_{\max}$ ,  $\gamma$ ,  $\Omega$ , and  $\mu$  necessary to calculate  $\Delta b_1$  were obtained by using data from recording instruments. The data in the form of  $\frac{\Delta b'}{\Delta b_1}$  are plotted in figure 7 against  $\frac{\theta}{C_T/\sigma}$ . The flight values of  $\theta$  and  $\frac{C_T}{\sigma}$  were also obtained through the use of data from recording instruments. Equation (9) is plotted for comparison. The horizontal dashed line at  $\frac{\Delta b'}{\Delta b_1} = 1.0$  represents damping as would be calculated if the rotor-force-vector tilt were assumed equal to tip-path-plane tilt.

## DISCUSSION

Comparison between the data of figure 7 and the line at  $\frac{\Delta b'}{\Delta b_1} = 1.0$  confirms the theoretical prediction that calculations of rotor damping based on the tilt of the tip-path plane are not necessarily correct (even approximately). The data also confirm the theoretical prediction that the ratio of rotor-force-vector tilt to calculated tip-path-plane tilt due to damping in pitch or roll depends primarily upon and decreases with increasing value of the parameter  $\frac{\theta}{C_T/\sigma}$ . Extrapolation of the flight data also confirms the theoretical prediction that rotor damping becomes unstable above a value of  $\frac{\theta}{C_T/\sigma}$  of about 3. The relatively small discrepancy between the data and the theory appears to be due primarily to changes in induced velocity which occur during rolling because of changes in the distribution of thrust around the rotor disk. These changes in induced velocity are not taken into account in the theoretical calculations because of the excessive labor that would be involved.

Because of the effect of the parameter  $\frac{\theta}{C_T/\sigma}$  on rotor damping, it is of interest to point out the variations in the magnitude of this parameter with variations in flight condition. For a given value of  $\frac{C_T}{\sigma}$ , the value of  $\theta$  increases with increasing level-flight speed (above the speed for minimum power) and with increasing rates of climb. Thus, the high-damping test points on the left-hand side of figure 7 represent autorotation, whereas the low-damping test points on the right-hand side represent full-throttle climb and high-speed level flight. It would therefore be expected that the high-speed high-powered helicopter would tend to have unstable damping in pitch and roll. Also, a convertible aircraft, the lifting rotor of which has flapping hinges and is used for high-speed propulsion, would be expected to have unstable damping because of the necessarily high value of  $\frac{\theta}{C_T/\sigma}$ .

In order to obtain a more definite idea of the seriousness of this problem for the high-speed helicopter, a preliminary design of a high-speed helicopter was made. The specifications for this helicopter were set as follows:

$$V_{\max} = 270 \text{ feet per second} \approx 185 \text{ mph}$$

Altitude, sea level

$$W = 7000 \text{ pounds}$$

$$\frac{W}{\pi R^2} = 2.3$$

Untwisted blades

Fuselage parasite area, 15 square feet (about one-half the value for a present-day 5000-pound machine)

A minimum tip-speed ratio  $\mu$  of 0.45 is necessary to prevent the advancing blade tip from exceeding a Mach number of 0.8. The value of  $C_L$  is calculated to be 0.027.

By means of the performance charts of reference 5, the minimum rotor solidity necessary to prevent stalling of the retreating blade tip is found to be approximately 0.10. The power required is then found to be approximately 1250 horsepower, the value of collective pitch  $\theta$  is approximately 0.15 radians, and the value of  $C_T/\sigma$  is approximately 0.027.

The value of the parameter  $\frac{\theta}{C_T/\sigma}$  is then found to be approximately 5.6.

From figure 7, extrapolation indicates that, at this value of  $\frac{\theta}{C_T/\sigma}$ , the

rotor damping of the high-speed helicopter would be highly unstable. This amount of unstable damping is probably intolerable.

Figure 7 also indicates the possibility of trouble even for present-day helicopters. During steady flight, the test helicopter has achieved values of  $\frac{\theta}{C_T/\sigma}$  of over 2.4 in steady high-speed level flight. If, at this flight condition, a maneuver were performed (either intentionally or inadvertently) which resulted in a reduction of normal acceleration below 1 g, the parameter  $\frac{\theta}{C_T/\sigma}$  would increase because of the reduction in thrust. For example, a reduction to  $\frac{1}{2}g$  while constant rotor speed is maintained would raise  $\frac{\theta}{C_T/\sigma}$  from 2.4 to 4.8 where the rotor damping is highly unstable. Since many present-day helicopters are unstable with angle of attack, the recovery from such a maneuver could be extremely difficult to make.

Because of this tendency of the helicopter rotor toward unstable damping, some special effort must be made to design adequate rotor damping into the high-speed high-powered helicopter. The use of a rate gyroscope or similar device which would apply opposite cyclic control to the rotor during rolling or pitching is one possible solution; however, these devices tend to be limited, for mechanical reasons, in the amount of control they can apply. Another possibility is the use of offset flapping hinges. Figure 8 shows that with offset hinges, a tilt of the rotor tip-path plane will produce a moment about the helicopter center of gravity in the direction of the tilt because of the mass forces in the blades. Thus, inasmuch as the tip-path plane always tilts opposite to the pitching or rolling velocity, the use of offset hinges would provide a source of stable damping to counteract the unstable damping tendency of the conventional rotor operating at high values of  $\frac{\theta}{C_T/\sigma}$ . Calculations indicate that, for the high-speed helicopter discussed previously, offsetting the flapping hinges about 10 percent of the rotor radius would make the resulting rotor damping about equal to the stable damping of the test helicopter at low-speed level flight (circled test points of fig. 7), which is relatively satisfactory.

Although this investigation has been restricted to the single-rotor helicopter, the ideas can be applied to a twin-rotor helicopter as well. Thus, a tandem helicopter acts as a single-rotor machine during rolling; whereas, a side-by-side helicopter acts as a single-rotor machine during pitching.

The equations of this paper can be applied to rotors having twisted or tapered blades. The effect of a linear twist in the blades can be accounted for by basing  $\theta$  on the pitch at  $\frac{3}{4}B$  of the radius.

Calculation for rotors with blades having typical amounts of taper can be made adequately by determining  $\sigma$  and  $\gamma$  as shown in the section entitled "Symbols."

It has recently been noted that an analysis similar to the one presented herein but restricted to the hovering condition is included in reference 6. The equations of this reference can be reduced to the form of the equations presented herein for  $B = 1.0$  and  $\mu = 0$ ; thus, an independent check of the integrations involved is provided. However, since the analysis of reference 6 was restricted to hovering, no mention was made of the large variations in damping with change in flight condition nor of the possibility of unstable damping.

### CONCLUSIONS

As a result of theoretical calculations confirmed by flight-test measurements of rotor damping for a single-rotor helicopter with conventional control system, the following conclusions are drawn:

1. The damping moment about the helicopter center of gravity during steady pitching or rolling supplied by a rotor, the flapping hinges of which are on the rotor shaft, depends primarily upon four quantities: rotor speed, blade-mass factor, height of the rotor hub above the helicopter center of gravity, and the ratio of collective pitch to the thrust coefficient-solidity ratio  $\frac{\theta}{C_T/\sigma}$ .
2. The damping moment per unit angular velocity is inversely proportional to rotor speed and blade-mass factor and directly proportional to hub height. For a given helicopter, these quantities are relatively constant. The damping moment decreases linearly with increasing value of  $\frac{\theta}{C_T/\sigma}$  and becomes unstable (moment in the same direction as the angular velocity) above a value of  $\frac{\theta}{C_T/\sigma}$  of about 3 when  $\theta$  is in radians.
3. Present-day helicopters with conventional control systems tend to have low damping at high speed and in climbs and can even have unstable damping when in a maneuver during which the normal acceleration falls well below 1 g.
4. High-speed high-powered helicopters and those convertible aircraft, the lifting rotors of which have flapping hinges and are used for high-speed propulsion, will have intolerable amounts of unstable rotor damping because of the necessarily high values of  $\frac{\theta}{C_T/\sigma}$  unless special design features,



such as offset flapping hinges or a rate gyroscope applying opposite cyclic pitch control proportional to the angular velocity are used.

5. Results of damping-moment calculations that assume the rotor-force-vector tilt to be equal to the tip-path-plane tilt during rolling or pitching (often done for convenience) may be highly misleading.

Langley Aeronautical Laboratory  
National Advisory Committee for Aeronautics  
Langley Air Force Base, Va., May 15, 1950

#### REFERENCES

1. Reeder, John P., and Gustafson, F. B.: On the Flying Qualities of Helicopters. NACA TN 1799, 1949.
2. Gessow, Alfred, and Amer, Kenneth B.: An Introduction to the Physical Aspects of Helicopter Stability. NACA TN 1982, 1949.
3. Den Hartog, J. P.: Mechanical Vibrations. Third ed., McGraw-Hill Book Co., Inc., 1947.
4. Wheatley, John B.: An Aerodynamic Analysis of the Autogiro Rotor with a Comparison between Calculated and Experimental Results. NACA Rep. 487, 1934.
5. Bailey, F. J., Jr., and Gustafson, F. B.: Charts for Estimation of the Characteristics of a Helicopter Rotor in Forward Flight. I - Profile Drag-Lift Ratio for Untwisted Rectangular Blades. NACA ACR L4H07, 1944.
6. Miller, R. H.: Helicopter Control and Stability in Hovering Flight. Jour. Aero. Sci., vol. 15, no. 8, Aug. 1948, pp. 453-472.

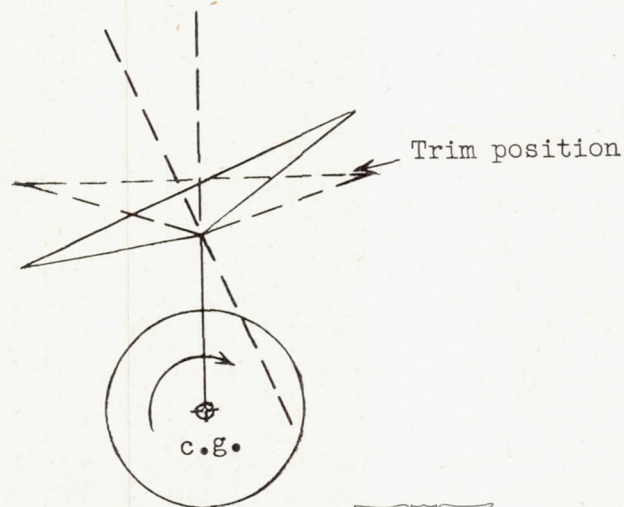


Figure 1.- Source of damping in roll for a helicopter undergoing a rolling velocity.

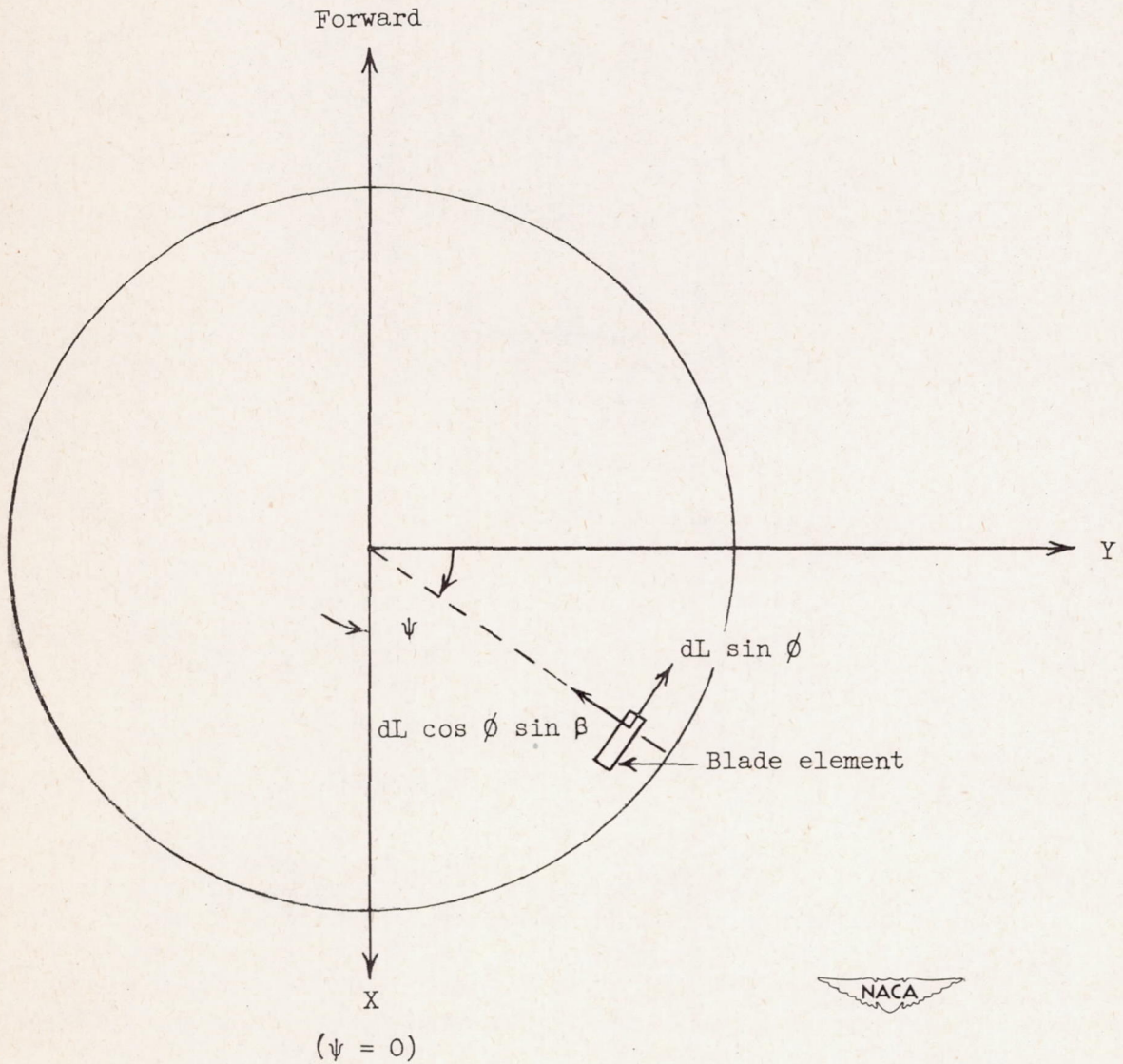


Figure 2.- Origin of the lateral-force contribution of the lift acting on a rotor-blade element.  $(dY = (dL \sin \phi)\cos \psi - (dL \cos \phi \sin \beta)\sin \psi)$

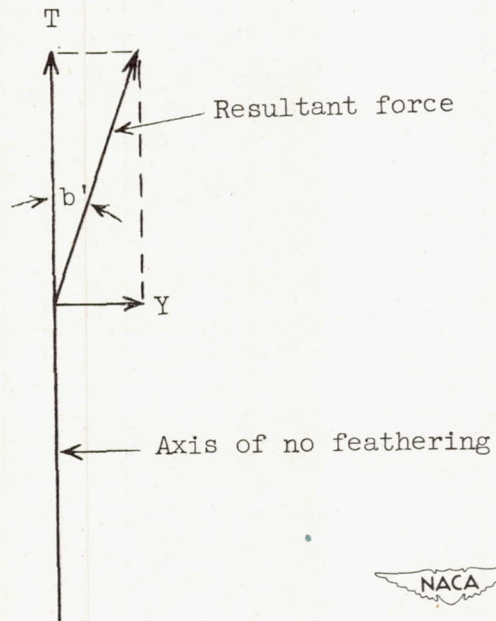
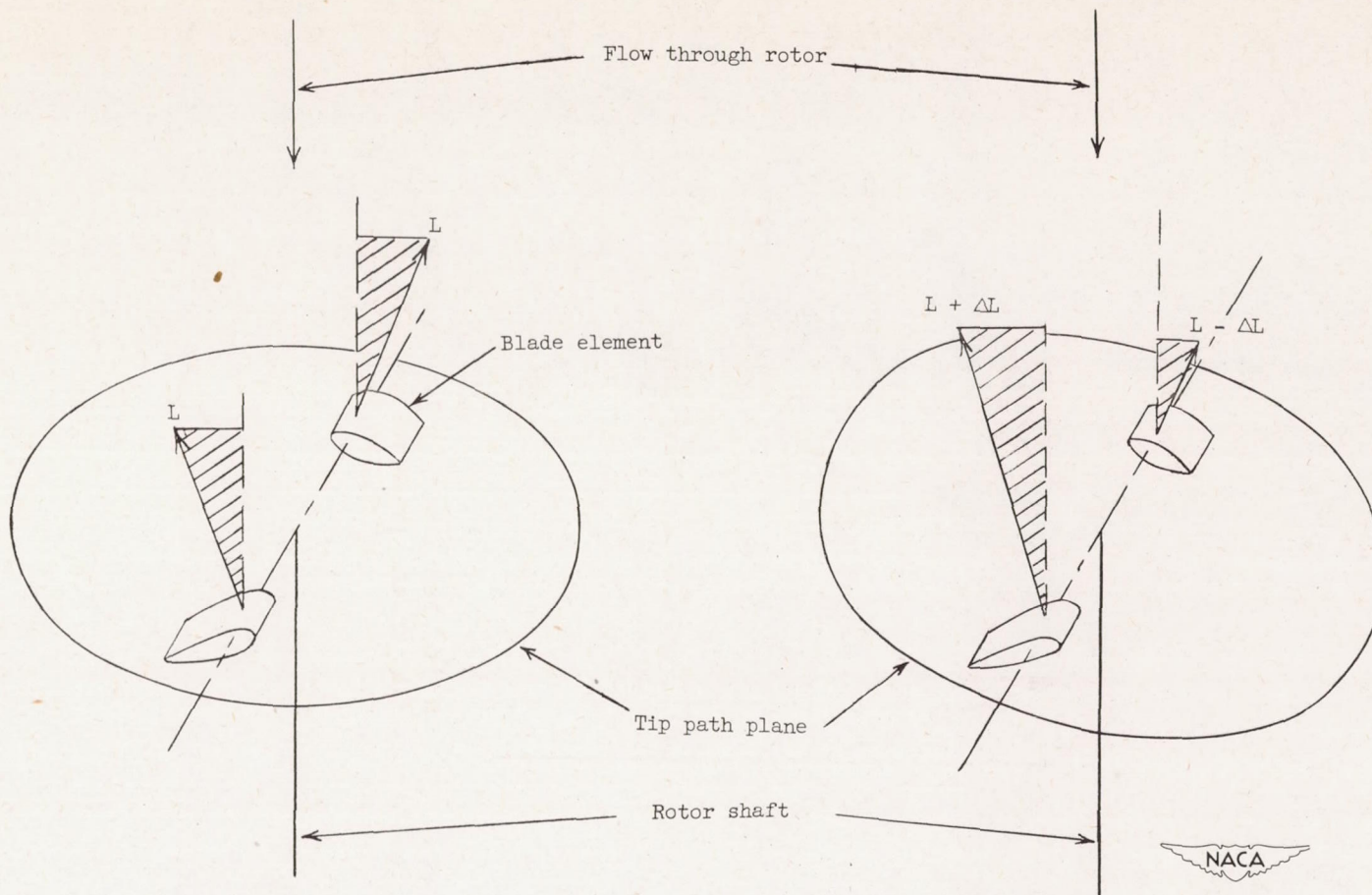


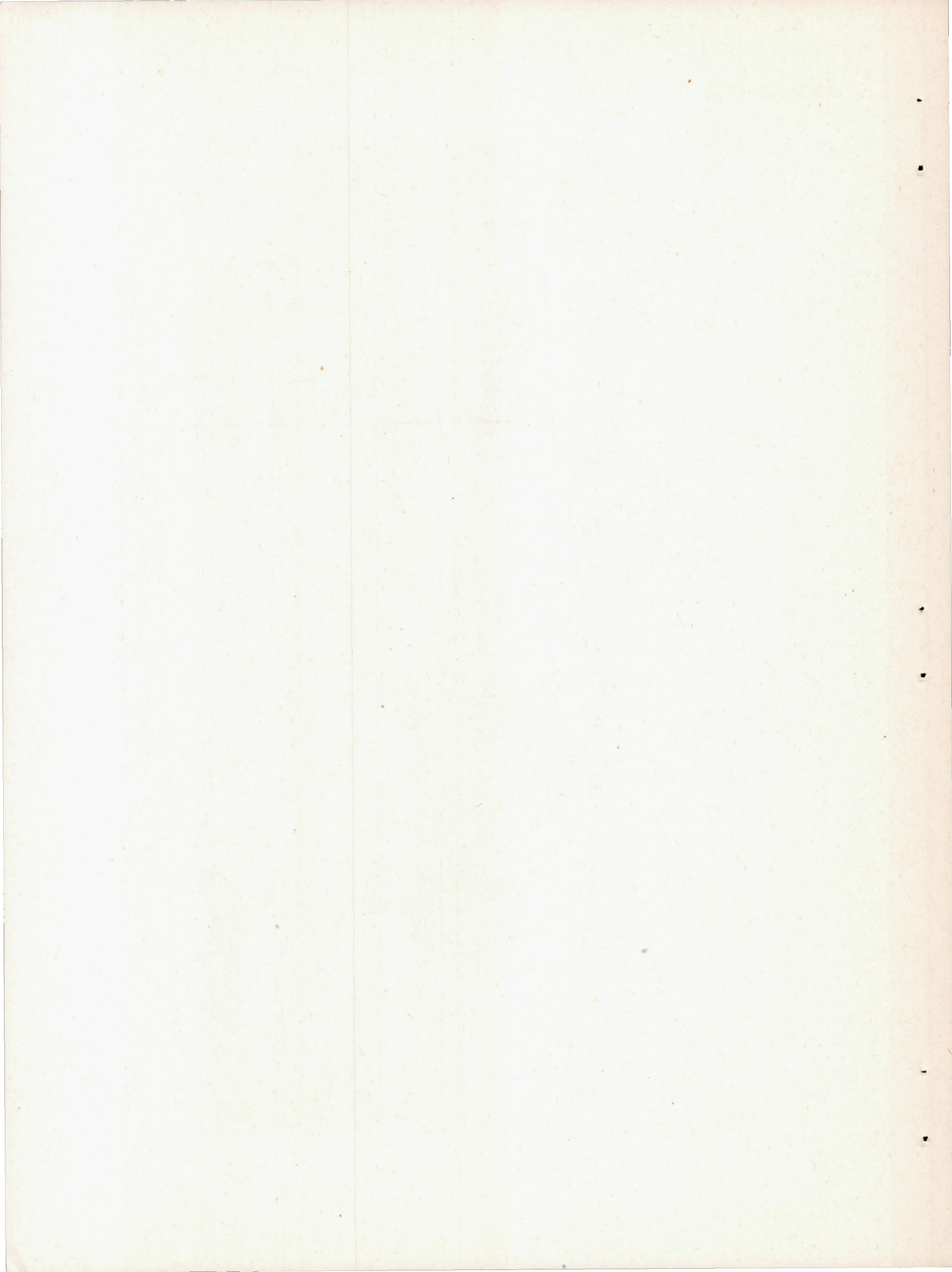
Figure 3.- Lateral tilt of the resultant rotor-force vector from the axis of no feathering due to the presence of a lateral force  $Y$ .



(a) Trim condition.

(b) Roll to the left.

Figure 4.- Source of unstable rotor damping in roll. The rotor is being viewed from the tail of the helicopter. The airfoil sections are typical sections of the blades when in the forward and rearward position.



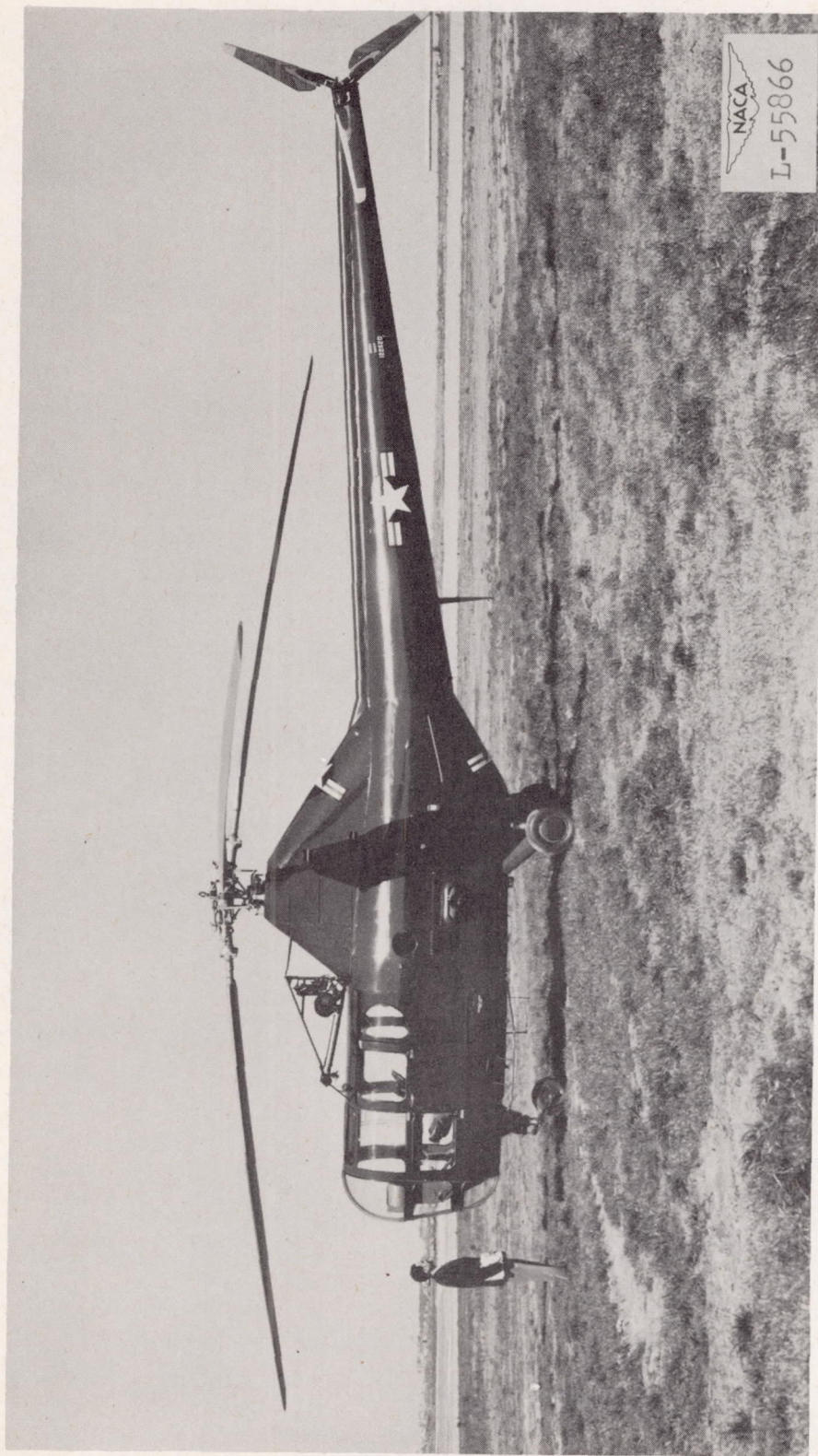
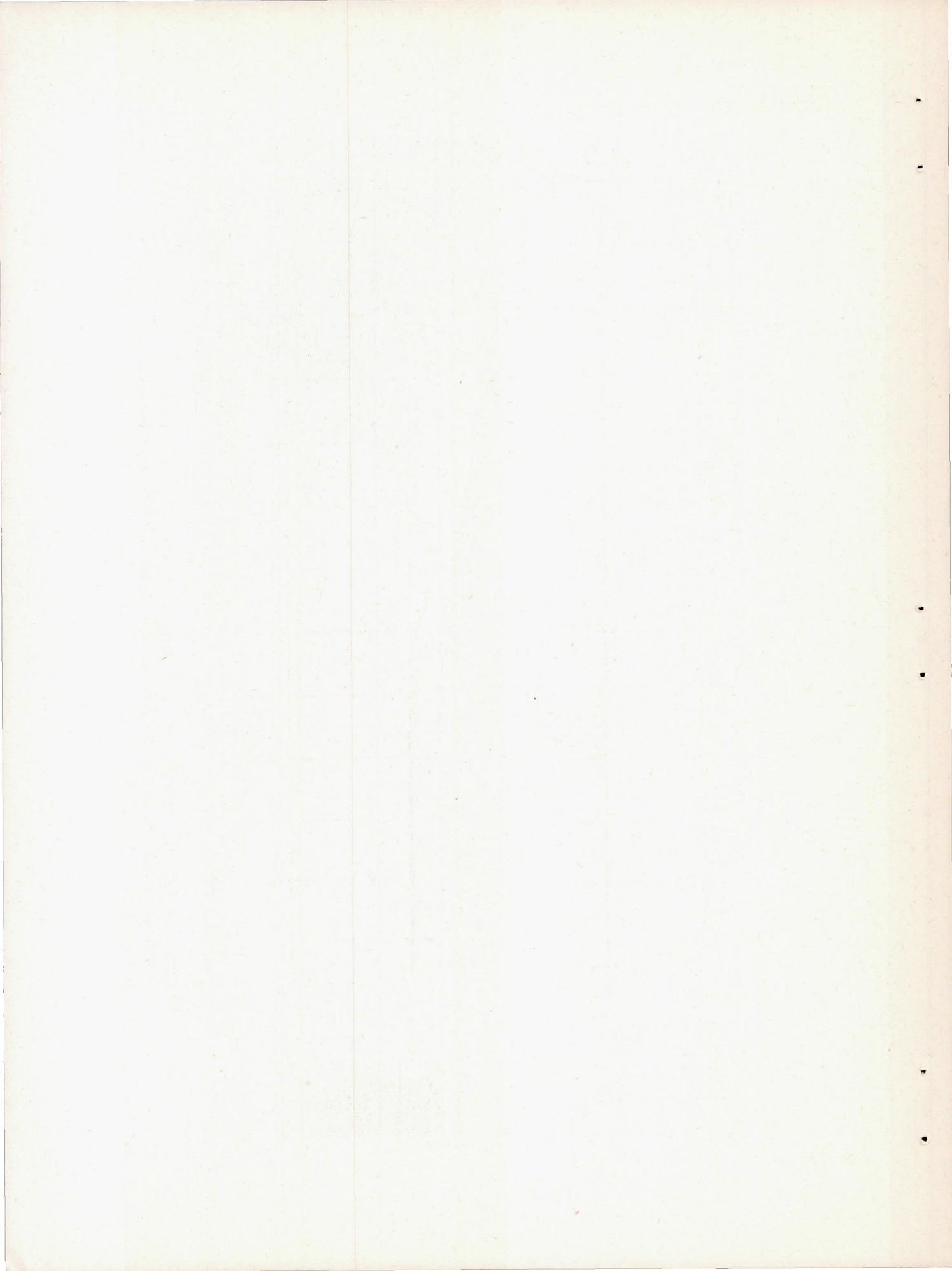
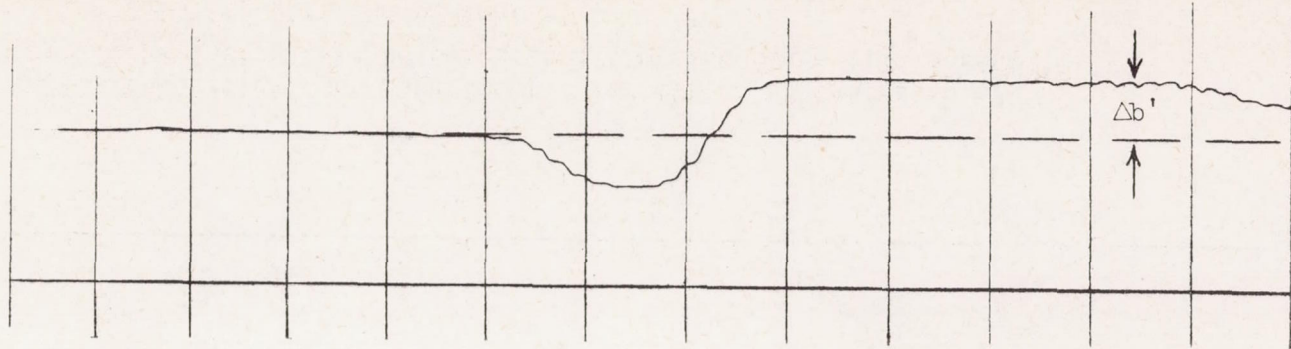


Figure 5.- Test helicopter.





Lateral cyclic pitch from trim 0



Rolling velocity 0

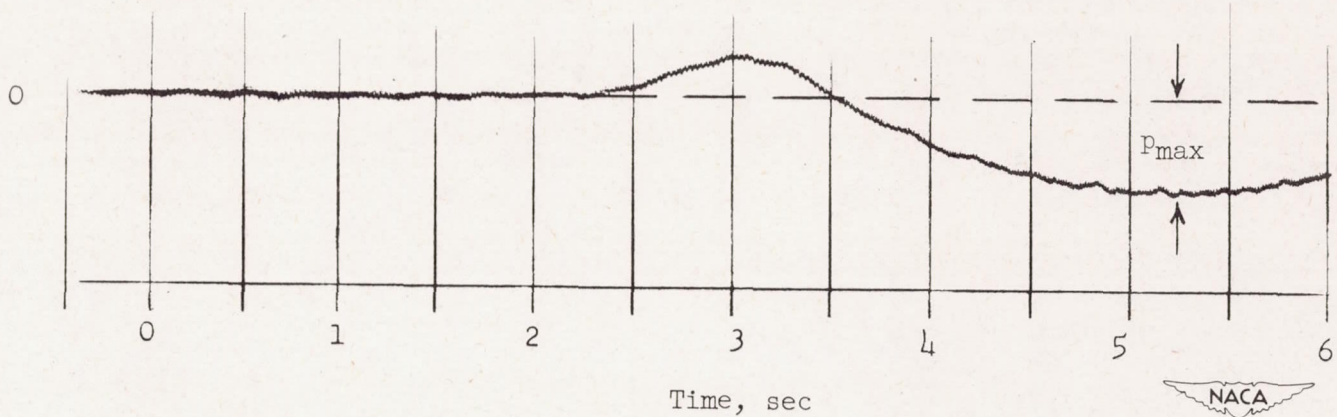


Figure 6.- Typical records of the time histories of lateral cyclic-control position and rolling angular velocity during the test maneuvers.



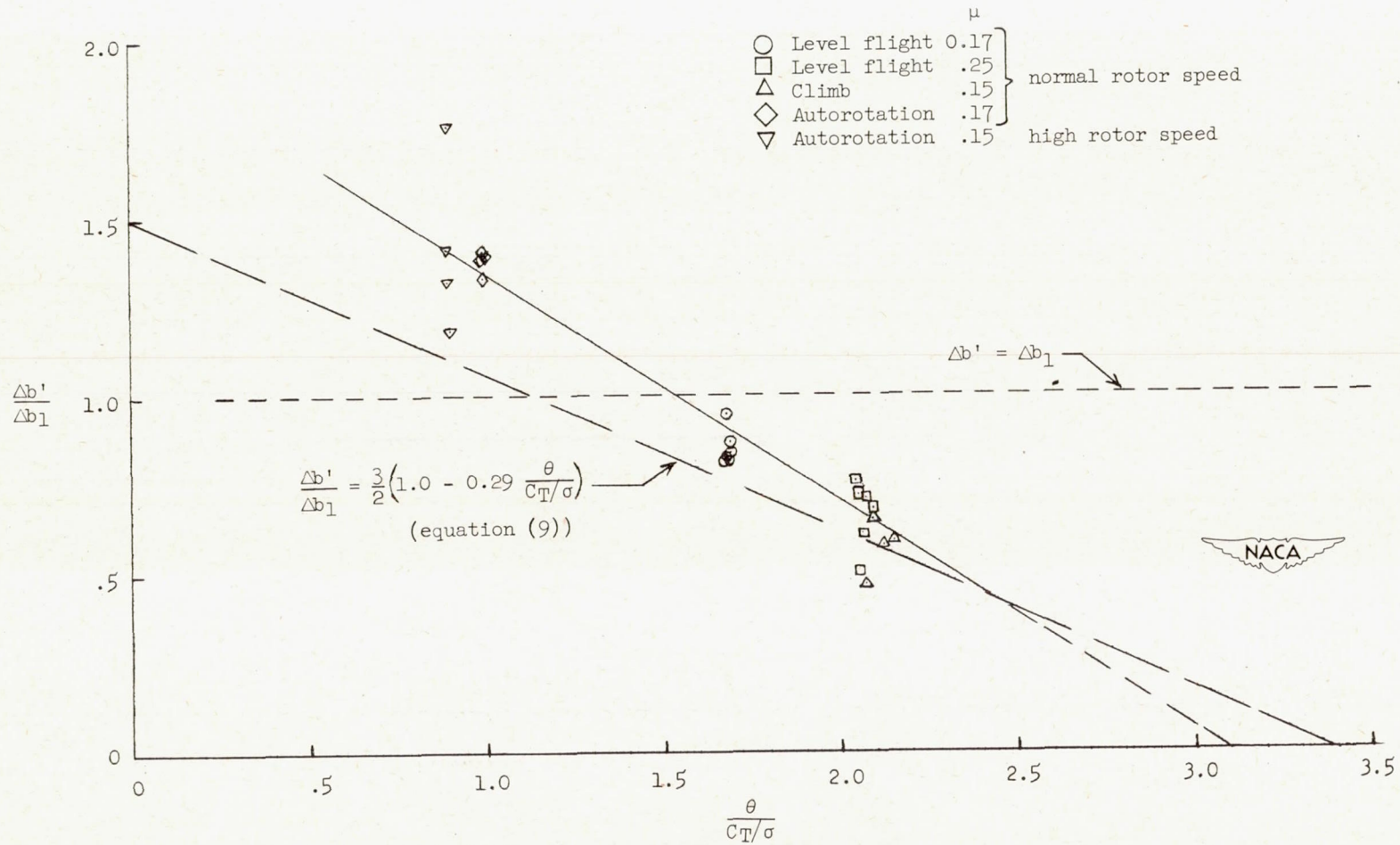


Figure 7.- Theoretical and experimental variations of the ratio of rotor-force-vector tilt to calculated tip-path-plane tilt during rolling velocity with the parameter  $\frac{\theta}{C_T/\sigma}$ .

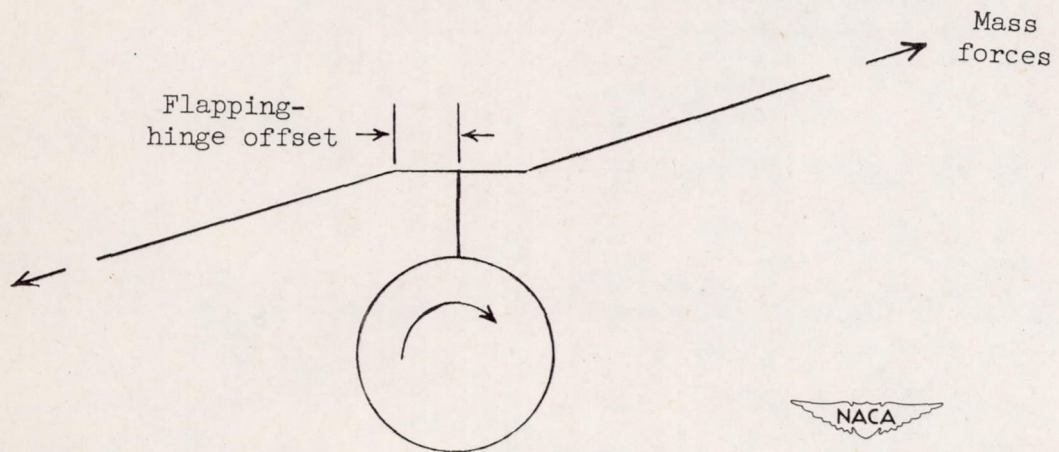


Figure 8.- Source of the stable damping contribution of the rotor due to offset flapping hinges.

